Correlating heterogeneous production to seismic curvature attributes in an Australian coalbed methane field.

Jeremy C. Fisk, Kurt J. Marfurt, The University of Oklahoma, Dennis Cooke, Santos, Ltd.*

Summary

Australia is the world's second largest producer of coalbed methane (Faiz, 2008). Characterized as a marginal tectonic setting, the Bowen Basin of Queensland displays a thick succession of numerous thin bituminous rank coal seams. The area's heterogeneous production is particularly perplexing; it is not unusual for production to change as much as 50-75% between neighboring wells within a few kilometers of one another. A myriad of factors can affect coalbed methane production to include coal thickness, coal cleat architecture, local maximum horizontal stress direction, and the *in situ* stress magnitude.

We show how seismic curvature attributes illustrate lineaments that correlate to production. We use a technique to generate 3D rose diagrams from curvature attributes and show that the diagrams depict the face and butt cleat architecture.

Introduction

Unconventional reservoirs continue to contribute an increasing percentage of the total amount of oil and gas production in the world. Shale and coal are examples of low-permeability unconventional reservoirs that often act as both the primary source rock and the reservoir. The application of seismic attributes and multiattribute transforms are incrementally pushing the limits to seismic resolution and facilitating different data analysis perspectives to use during reservoir characterization.

Geologic Background

The Bowen Basin is a Permian-Triassic age major economic coal basin that extends approximately 900 km in a generally north to south direction in the eastern portion of Queensland, Australia. The Bowen Basin is one portion of the Bowen-Gunnedah-Sydney foreland system that formed as a result of the collision of the paleo-Pacific and paleo-Australian plates beginning as early as 294 Ma in the Early Permian. This orogenic belt is often referred to as the New England fold belt. Figure 1 is a map of Australia which outlines the approximate geographical limits of the Bowen Basin in Queensland.

Toward the end of the Permian, the coal measures formed in environments described as fluvio-deltaic. Structurally, this reservoir lies within a large anticlinal structure that Korsch (2004) has labeled a fault-propagation fold.

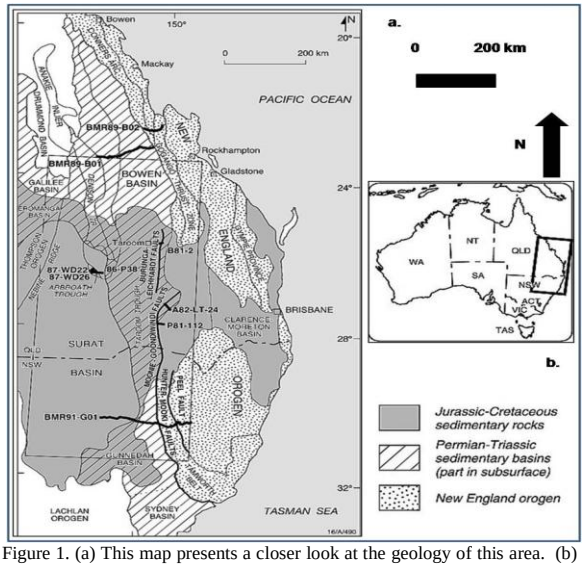

Figure 1. (a) This map presents a closer look at the geology of this area. (b) The black box surrounds the location of the Bowen and Surat Basins in Australia. The Bowen and Surat Basins contain more than 70 small commercial oil and gas fields. Many of these fields are in anticlines that formed due to the New England orogen thrusting (Korsch, 2004).

Figure 2 is a seismic inline view of the fault propagation fold from the 3D seismic data for this study with interpreted faults. Figure 3 shows the seismic line (A-A') from Figure 2 and well production data for this 3D seismic survey.

Seismic Data Quality

The company's primary goal for this 3D seismic survey was the improved mapping of the upper coal horizons within the basin. The survey size is 31.56 km^2 of rolling farmlands. The data were recorded using 45 source lines with a 200 m interval and 23 receiver lines with a 200 m interval, resulting in a natural bin spacing of 25 m x 12.5 m. Four Mertz M26 vibrators vibrated with a sweep length of four seconds and a sweep frequency range from 6-130 Hz. Group arrays consisted of twelve sensor SM4, 10 Hz geophones in a linear array with the source in the middle of each line, resulting in a multiplicity of 36 fold. The sampling rate of the data is 2 ms. Some pre-stack processing parameters were surface consistent deconvolution, 10-110 Hz spectral whitening, and spatial dealiasing DMO. Some of the final post-stack parameters were spectral balancing 10-110 Hz, F/X deconvolution, and modified residual migration with 100% smoothed velocities.

Heterogeneous production in a CBM field

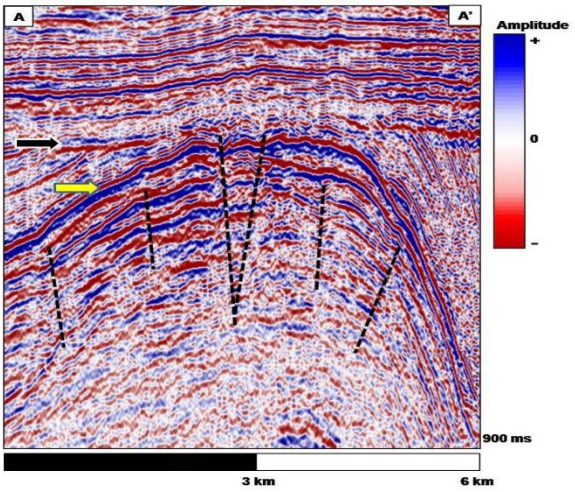

Figure 2. The coalbed methane reservoir lies within this prominent anticline. The yellow block arrow points at the top coal seam (a strong negative amplitude). The black block arrow points to the visible unconformity that separates the Triassic and Jurassic time periods. The black dashed lines are interpreted faults that have formed as a result of the folding in this area.

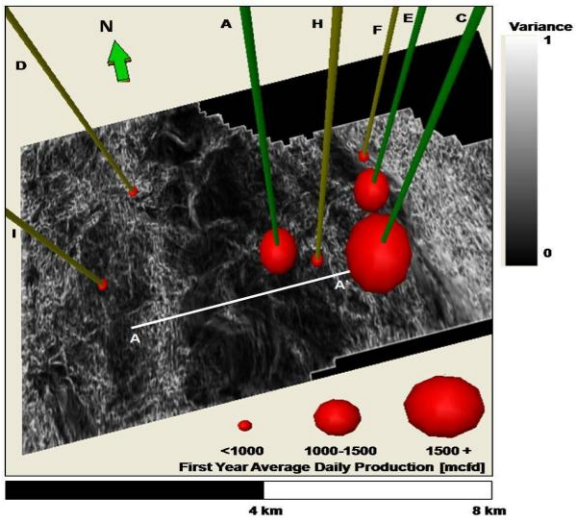

Figure 3. A time slice of the variance cube depicting the wells in the study area. The A – A' line is the vertical section in Figure 2. The first year average daily production for the wells in million cubic feet per day are depicted with the bubbles. The name of each well is listed to the left of the wellbore.

Previous Studies

Marroquin and Hart (2004) use seismic attributes to map lineaments in coal and correlate production to those seismic lineaments in the Fruitland Formation. McCrank and Lawton (2009) present a seismic study that includes seismic horizon interpretations and an acoustic impedance inversion of Ardley coals in Canada. Chopra et. al (2009) use curvature azimuth and shape- revealing attributes to generate 3D rose diagrams that assist in the interpretation of structural features and their potential connection to image logs or production. In addition, Nelson (2001) shows through outcrop and numerical methods that flexure-related fractures will be greatest at the location of maximum curvature.

Theory and Method

Cleats

Cleats are the natural fractures that develop in coal as a result of factors such as dehydration, differential compaction, and paleotectonic stresses (Close,1993). Two main sets of cleats that form in coalbeds are face cleats and butt cleats. Face cleats are typically the primary cleat set, are the tallest and longest cleats in the coalbed, and are the first fractures to form in the coal (Grout,1991). Butt cleats are the secondary cleat system that are orthogonal to the face cleats and perpendicular to bedding (Solano-Acosta et al., 2007). Figure 4 depicts a typical array of cleats within a coalbed. Cleats provide the main permeability pathway in coals for Darcy flow of gas and water.

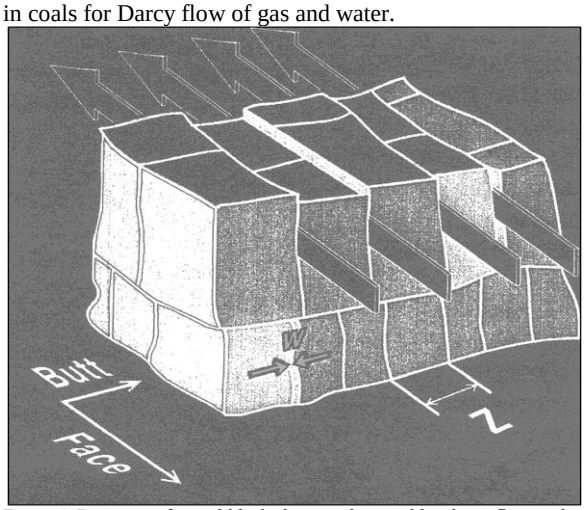

Figure 4. Depiction of a coal block showing the variables that influence the fracture permeability (Nelson, 2001) in coal defined by the equation $k_F=w^3/(12*z)$, where k_F is the fracture permeability, w is the cleat aperture width, and z is the average cleat spacing (Modified after Scott, 2000).

Curvature

Volumetric curvature seismic attributes gauge the lateral variability in dip magnitude and dip azimuth (Mai et al., 2009). Curvature in three dimensions represents the values of the radii of two orthogonal circles fit tangent to a surface. Since curvature, k, is equal to the reciprocal of the radius of curvature for these circles, k_{min} represents the circle that fits tangent to the surface with the largest radius and k_{max} is the other circle tangent to the surface with the smallest radius (Chopra and Marfurt, 2007). Figure 5 provides a visualization of the relationship between

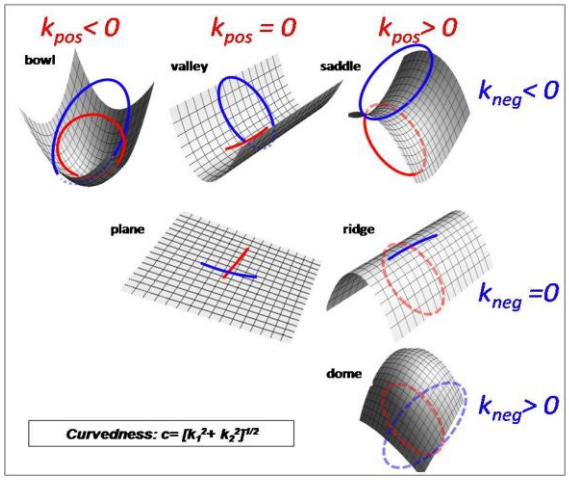

Figure 5. This figure defines 3D quadratic shapes in terms of most-positive, k_{pos} , and most-negative curvature, k_{neg}. Synclinal features have negative curvature values for k_{pos} and k_{neg}. Anticlinal features have positive curvature values for k_{pos} and k_{neg}. For a plane, both k_{pos} and k_{neg} have values of zero (After Mai, 2010).

curvature and geologic features in a 3D reference frame. The mathematical calculation of curvature from an interpreted surface requires fitting a quadratic surface, *z(x,y)*, to a window of data points. The resulting principal curvatures are computed from first and second derivatives of these picks. Volumetric *structural* curvature is similar, but replaces the first derivative calculations with volumetric estimates of the inline and crossline dip (Marfurt, 2010). Chopra et al. (2009) point out that most positive and most negative principal curvatures are the most effective in "mapping subtle flexures and folds associated with fractures in deformed strata." In volumetric *amplitude* curvature calculations, the first derivative calculations are replaced by volumetric estimates of the inline and crossline gradients as directional measures of amplitude variability (Chopra and Marfurt, 2007).

Shape Index modulated by Curvedness

Curvedness provides a measure of the intensity of structural deformation at a given point. Chopra and Marfurt (2007) define the curvedness, *c*, of a surface as:

$$c = \left[(k_1^2 + k_2^2)/2\right]^{1/2}, \quad (1)$$

where k_1 is the maximum principal curvature and the minimum principal curvature is k_2. These principal curvatures measure the maximum and minimum bending of the surface at each point (Lisle, 1994). Chopra and Marfurt (2007) define the shape index, *s*, as:

$$s = \frac{2}{\pi} tan^{-1}\left[\frac{k_2+k_1}{k_2-k_1}\right]. \quad (2)$$

The result of the shape index is a seismic attribute volume whose amplitudes correspond to shapes, where the shape index of a dome is 1.0, a ridge is 0.5, a saddle is 0.0, a valley is -0.5, and a bowl is -1.0. When the shape index is co-rendered in a seismic display with curvedness, high curvedness values that correspond with ridge and valley shape indices are directly related to lineaments (Chopra et al., 2009).

3D Rose Diagrams

Estimation of face and butt cleat orientation is critical to planning wellbore trajectory and completion procedures. Since the resolution of my seismic survey is limited to about 8 m, we need to use an indirect approach in determining the orientation of cleats. Multiple studies have determined that coal butt and face cleats, having apertures on the order of millimeters, are correlated to the regional fracture geometry. Nelson (2001) found that regional fractures usually parallel cleat directions, with face cleats corresponding to the systematic regional fracture set and butt cleats the non-systematic regional fracture set. Grout (1991) notes that cleats in the southern Piceance basin correlate to fractures in overlying clastic rocks.

We determine the fracture set orientations seismically through the generation of 3D rose diagrams. In this process, a seismic volume is binned in even squares of 250 m x 250 m. Then, the magnitude of a given rose petal at a single horizon is defined by the summed and scaled ridge or valley component of curvature values within a bin. The strike direction of the rose petal is defined by the value for the strike of minimum curvature, which is the axis of the folding plane. More details for this process are documented in Chopra et al. (2009).

Discussion and Results

Using image logs from wells in the survey area and borehole breakouts, Johnson et al. (2002) determined the maximum horizontal stress, $\sigma_{H\text{-}Max}$, of the survey area to be northeast. Cleats and fractures aligned parallel or near parallel to the maximum horizontal stress are more likely to be open and are likely to be the face cleats. Conversely, cleats and fractures aligned perpendicular to the maximum horizontal stress are more likely to be closed. Marfurt et al. (2009) suggest that the ridge component is better to use in compressional regimes, and the valley component is better to apply in extensional environments. We first consider the most-positive curvature attribute to illuminate anticlinal features that may be highlighted as result of the thrust system in this 3D seismic survey. Figure 6 is the most positive amplitude curvature with high red curvature values indicating anticlinal features or ridges. We investigate the fracture orientations near the top coal horizon with the 3D rose diagrams. We expect that better producing wells

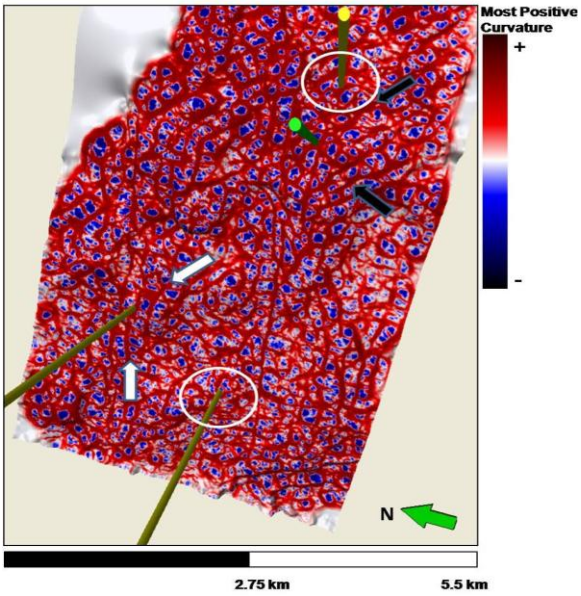

Figure 6. This view of the top coal seam through the most positive amplitude curvature volume. High values (red) can indicate anticlinal features or ridge-like lineaments. The high producer (well A) shows strong most positive curvature trends (black block arrows) from orthogonal directions leading to the wellbore. The surrounding low producers do not show this same trend (white block arrows and circles).

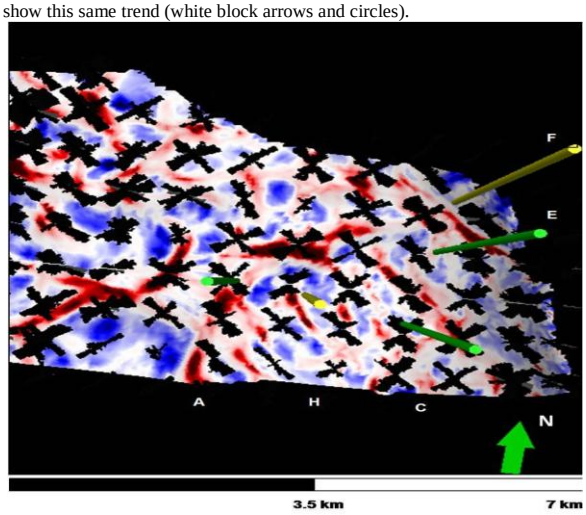

Figure 7. This map view of the top coal seam shows the 3D rose diagrams at the respective well locations. The rose diagrams show strong bi-directional trends at higher producing wells A and C, and lower producing wells H and F show a more uni-directional trend.

will show a strong presence of fractures oriented parallel to $\sigma_{H\text{-}Max}$. Figure 7 is the top coal surface with the 3D rose diagrams overlain. This image reveals that the higher producing wells A and C show a strong bi-directional trend, suggesting that contributions from both systematic and non-systematic fracture sets or a strong presence of face and butt cleats may be contributing to the wells' deliverability. Furthermore, rose diagrams of the lower producing wells H and F show a more uni-directional trend.

The shape index co-rendered with curvedness (Figure 8) provides additional insight into the topography of the top of the coal seam. Figure 8 shows the areas of high curvedness and intense structural deformation that correspond with different shapes, most notably ridge features associated with compressive stress regimes.

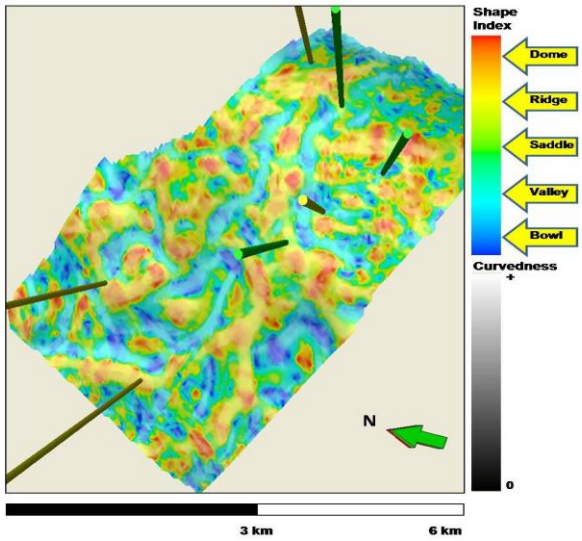

Figure 8. The top coal displayed as the shape index co-rendered with the curvedness. The areas with greater curvedness and more structural deformation appear with white undertones.

Conclusions

Seismic curvature attributes are effective at mapping features that relate to production in coals. Bi-directional, orthogonal lineaments in the 3D rose diagrams show areas of enhanced permeability and higher production. We interpret this to be due to a strong presence of face and butt cleats. The amplitude curvature volume reveals most-positive, ridge-like trends along the maximum and minimum horizontal stress directions leading to the wellbore of a high producing well. Low-producing wells reveal weak, amplitude curvature lineaments in the vicinity of the well locations. Finally, the shape index co-rendered with the curvedness allows the interpreter to map surface topography and identify areas associated with heightened structural deformation.

Acknowledgements

We would like to thank Santos, Ltd. for providing all of the data for this study, the University of Oklahoma AASPI consortium for the software to generate the different curvature volumes, and Schlumberger for visualization.